

## RESEARCH ARTICLE

# Visual pathway neurodegeneration winged by mitochondrial dysfunction

Axel Petzold<sup>1,2,3,10</sup>, Philip G. Nijland<sup>4</sup>, Lisanne J. Balk<sup>1</sup>, Angela Maria Amorini<sup>5</sup>, Giacomo Lazzarino<sup>5</sup>, Mike P. Wattjes<sup>6</sup>, Claudio Gasperini<sup>7</sup>, Paul van der Valk<sup>4</sup>, Barbara Tavazzi<sup>5</sup>, Giuseppe Lazzarino<sup>8</sup> & Jack van Horsen<sup>9</sup>

<sup>1</sup>Department of Neurology, VU University Medical Center, De Boelelaan 1117, 1081 HV, Amsterdam, The Netherlands

<sup>2</sup>Department of Ophthalmology, VU University Medical Center, De Boelelaan 1117, 1081 HV, Amsterdam, The Netherlands

<sup>3</sup>Molecular Neuroscience, UCL Institute of Neurology, Queen Square, London, WC1N 3BG, United Kingdom

<sup>4</sup>Department of Pathology, VU University Medical Center, Amsterdam, The Netherlands

<sup>5</sup>Institute of Biochemistry and Clinical Biochemistry, Catholic University of Rome, Largo F. Vito 1, 00168, Rome, Italy

<sup>6</sup>Department of Radiology & Nuclear Medicine, VU University Medical Center, Amsterdam, The Netherlands

<sup>7</sup>Department of Neurosciences, S Camillo Forlanini Hospital, Circonvallazione Gianicolense 87, 00152, Rome, Italy

<sup>8</sup>Division of Biochemistry and Molecular Biology, Department of Biology, Geology and Environmental Sciences, University of Catania, Viale A. Doria 6, 95125, Catania, Italy

<sup>9</sup>Molecular Cell Biology and Immunology, VU University Medical Center, Amsterdam, The Netherlands

<sup>10</sup>Moorfields Eye Hospital, Neuro-ophthalmology, City Road, London, UK

## Correspondence

Axel Petzold, Departments of Neurology and Ophthalmology, VU University Medical Center, Amsterdam, De Boelelaan 1117, 1081 HV Amsterdam, NL and UCL Institute of Neurology, Molecular Neuroscience, Queen Square, London WC1N 3BG, United Kingdom. Tel: +31 204445292; Fax: +3120444 0715; E-mail: a.petzold@vumc.nl or a.petzold@ucl.ac.uk

## Funding Information

The MS Center VUMC is partially funded by a program grant of the Dutch MS Research Foundation (grant 09-358d MS). This work has partly been funded by the Catholic University of Rome and the University of Catania. Shipment of samples has been privately sponsored by A. P. The authors' work described in this article is supported by the University College London Comprehensive Biomedical Research Centre and the Moorfields Biomedical Research Centre.

Received: 12 September 2014; Revised: 29 October 2014; Accepted: 16 November 2014

*Annals of Clinical and Translational Neurology* 2015; 2(2): 140–150

doi: 10.1002/acn3.157

## Introduction

Understanding mechanisms driving progression of neurodegeneration in multiple sclerosis (MS) is relevant

## Abstract

**Objectives:** To test for structural and functional contribution of mitochondrial dysfunction to neurodegeneration in multiple sclerosis (MS). A visual pathway model *void* of MS lesions was chosen in order to *exclude* neurodegeneration secondary to lesion related axonotmesis. **Methods:** A single-centre cohort study (230 MS patients, 63 controls). Spectral domain optical coherence tomography of the retina, 3T magnetic resonance imaging of the brain, spectrophotometric assessment of serum lactate levels. Postmortem immunohistochemistry. **Results:** The visual pathway was *void* of MS lesions in 31 patients and 31 age-matched controls. Serum lactate was higher in MS compared to controls ( $P = 0.029$ ). High serum lactate was structurally related to atrophy of the retinal nerve fiber layer at the optic disc ( $P = 0.041$ ), macula ( $P = 0.025$ ), and the macular ganglion cell complex ( $P = 0.041$ ). High serum lactate was functionally related to poor color vision ( $P < 0.01$ ), Expanded Disability Status Scale score ( $R = 0.37$ ,  $P = 0.041$ ), Guy's Neurological disability score ( $R = 0.38$ ,  $P = 0.037$ ), MS walking scale ( $R = 0.50$ ,  $P = 0.009$ ), upper limb motor function ( $R = 0.53$ ,  $P = 0.002$ ). Immunohistochemistry demonstrated increased astrocytic expression of a key lactate generating enzyme in MS lesions as well as profound vascular expression of monocarboxylate transporter-1, which is involved in lactate transport. **Interpretation:** This study provides structural, functional, and translational evidence for visual pathway neurodegeneration in MS related to mitochondrial dysfunction.

for developing focused neuroprotective treatment strategies.<sup>1</sup> The most straightforward anatomical model is that axonal transection within active MS lesions causes distal axonal loss by Wallerian degeneration.<sup>2</sup> Once the axon is

lost and the neuron does not remain functionally connected, neuronal death follows a mechanism called dying back neuropathy. A more complex anatomical model is required to explain how axonal degeneration passes from a diseased to a healthy neuron. This is now understood to be a consequence of retrograde<sup>3,4</sup> and anterograde trans-synaptic axonal degeneration.<sup>5</sup> Truly, directionality of the process depends on localization of primary damage and will in most cases be bidirectional.<sup>6</sup> A physiological barrier to bidirectional trans-synaptic axonal degeneration is formed by anatomical structures capable of neuronal plasticity.<sup>6,7</sup> An important conclusion from these studies is that the substantial amount of retinal ganglion cell loss and axonal degeneration following episodes of MS associated optic neuritis (MSON) masks the more subtle degree of neurodegeneration attributable to more globally acting mechanisms.<sup>8,9</sup>

An important shortcoming of all optical coherence tomography (OCT) studies in the literature to date is that none excluded retinal layer atrophy to be a potential confounder of MS lesions in the optic pathways.<sup>4,10</sup> It may be possible that bidirectional trans-synaptic axonal degeneration does not explain all of the retinal layer atrophy seen

in MS. More global mechanisms are also present.<sup>11</sup> Therefore, to test these hypotheses using structural retinal imaging, one will need to be rigorous about excluding atrophy data from eyes with MSON and/or lesions within the posterior visual pathways.

But which are the molecular pathways that might lead to neurodegeneration on a more global level? Current understanding is that these consist of a cascade of events eventually leading to neuroaxonal degeneration as summarized in Figure 1. A common feature here is that a mitochondrial dysfunction is part of every single phase of this cascade of neurodegeneration.<sup>11–13</sup> As a result of mitochondrial dysfunction the cellular need for ATP is partly covered by conversion of pyruvate to lactate. This change from an aerobic to a nonaerobic metabolism leads to an increase of lactate levels.<sup>14</sup> Recent translational data directly relates neuronal loss to a dysfunctional aerobic energy metabolism.<sup>15</sup> An elegant quantitative method which permits to reach the cellular level in humans *in vivo* is spectral domain OCT.<sup>16</sup>

In order to prospectively test the hypothesis that patients with MS and mitochondrial failure suffer from more extensive neurodegeneration compared to patients

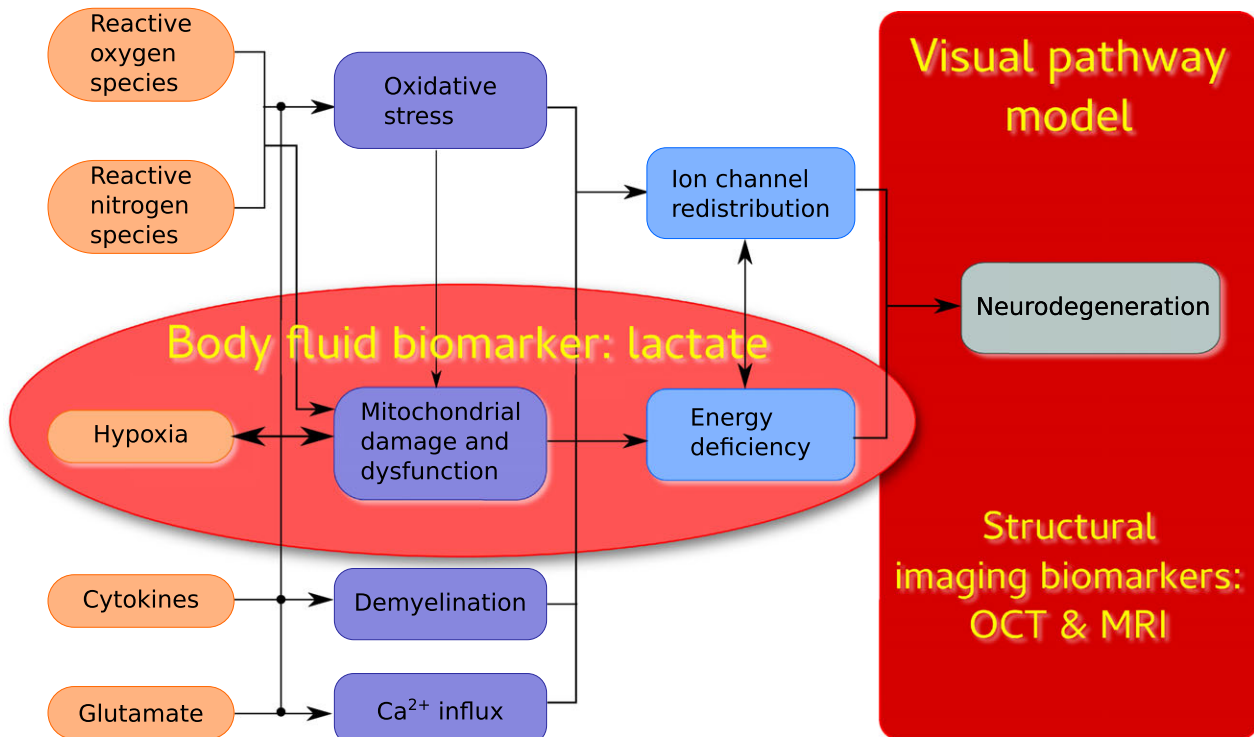


**Figure 1.** Prevailing hypotheses on molecular mechanisms leading to a cascade of events leading to more global neurodegeneration in the brain of patients with multiple sclerosis (MS) as could be expected from bidirectional trans-synaptic axonal degeneration alone. The red ellipse shows which of these mechanisms have in common, biochemically, that the anaerobic or impaired energy metabolism may cause an increase of systemic blood lactate levels, a body fluid biomarker. The red box highlights the visual pathway model used in this study using multimodal, structural imaging biomarkers.

with MS and no mitochondrial failure we took a combined body fluid biomarker and imaging biomarker approach. Because body fluid biomarker data can only ever provide indirect correlative evidence, postmortem immunohistochemical analyses were also performed. We hypothesized that patients with MS who had higher serum lactate levels compared to healthy controls will suffer from more extensive atrophy and loss of function.

## Methods

### Patients

This single centre cohort study was approved by the ethics committee of the VU University Medical Centre (protocol number 2010/336) and the scientific research committee (protocol number CWO/10-25D). Written, informed consent was obtained from all patients. All donors or their next of kin provided written informed consent for brain autopsy, use of material, and clinical information for research purposes. Inclusion criteria were age above 18 years and a diagnosis of clinically definite MS according to the original McDonald criteria.<sup>17</sup> Exclusion criteria were pregnancy, a relapse, or a course of steroids in the last 4 weeks, a diagnosis of HIV or other immunodeficiency, substance abuse in the past 5 years or MRI findings that could interfere with evaluation. For healthy controls additional exclusion criteria were any other neurological or psychiatric disease or a first or second degree relative with a diagnosis of MS. Episodes of MSON were identified through patient history and confirmed clinically using a standard care protocol.<sup>18</sup> The disease course was classified into relapsing remitting (RR), secondary progressive (SP) and primary progressive (PP).<sup>19</sup>

### Clinical scales

Physical disability was recorded on the Expanded Disability Status Scale score (EDSS), Guy's Neurological Disability Scale (GNDS), the Multiple Sclerosis Walking Scale (MSWS-12) and the 9-hole PEG test (9HPT) measuring upper limb motor function. For all scales a higher score indicates more disability. Snellen visual acuities (VA) were recorded and converted to decimal notation as recommended.<sup>18</sup> Color vision was tested using the Lanthony desaturated F15-hue test (D-F15d) with a daylight illuminator (6280°K) followed by validated, quantitative analyses.<sup>20</sup>

### Blood test

Blood samples were taken by antecubital venopuncture using a standard tourniquet procedure at time of the MRI. Samples were immediately spun down. Samples were then

alliquoted, coded, and stored in polypropylene tubes at  $-80^{\circ}\text{C}$  within 2 h of sampling. Serum samples were available from 192 of the 263 we have reported on before.<sup>7,21</sup> Serum lactate levels were measured spectrophotometrically (Agilent 89090A; Agilent Technologies, Santa Clara, CA).<sup>22</sup> The analyst was blinded to all other subject information.

### OCT and segmentation

Retinal OCT was performed as previously described.<sup>7,21</sup> In brief all images were obtained with a SD-OCT (Heidelberg Spectralis, software version 1.1.6.3, Heidelberg Engineering, Heidelberg, Germany) with the eye tracking function (EBF) enabled for best accuracy.<sup>23</sup> Data were collected from a peripapillary ring scan ( $12^{\circ}$ ) and a macular volume scan ( $20 \times 20^{\circ}$ ).

All scans underwent a rigorous quality control (QC) check.<sup>24</sup> From a total of 768 scans, 70 scans (9.1%) were excluded because they failed the validated OSCAR-IB QC criteria.<sup>24</sup> Automated segmentation was performed with the manufacturers software (HEYEX version 1.7.1.0, Viewing Module version 5.7.0.10, Heidelberg Engineering, Heidelberg, Germany). The peripapillary retinal nerve fiber layer (pRNFL), macular RNFL (mRNFL), and macular ganglion cell complex (mGCC) were taken for analysis.

### MRI acquisition

Structural magnetic resonance imaging (MRI) was performed on a 3T whole body system (GE Signa HDxt, Milwaukee, WI). The detailed acquisition parameters have been described previously as well as an example of the 3T MRI.<sup>7,21</sup> In brief, normalized gray and white matter volumes and lesion volumes were quantified automatically using k nearest neighbor classification with tissue type priors (KNN-TTP), and SIENAX (part of the FMRIB Software Library [FSL] 5.0.4, <http://www.fmrib.ox.ac.uk/fsl>). Lesion filling was applied to minimize the effect of lesions on atrophy measurements.

### Immunohistochemistry

White matter brain samples were obtained from seven MS patients (average age: 61, 57% male, 57% secondary progressive multiple sclerosis SPMS, average disease duration of 37 years) in collaboration with the Netherlands Brain Bank, Amsterdam, The Netherlands (coordinator Dr. Huitinga). Cryosections were used for detection of monocarboxylate transporter 1 (MCT1) (dilution 1:1000, kindly provided by Dr. Fishbein and Dr. Merezhinskaya).<sup>25</sup> Paraffin sections were used for detection of lactate dehydrogenase A (LDHA) (dilution 1:3000; Novus biologicals, Littleton, CO).<sup>26</sup>

## Data analysis

All statistical analyses were performed in SAS (version 9.3 SAS Institute Inc., Cary, USA). For statistical analyses the averaged OCT and D-F15d data of both eyes were used from each patient. In cases with unilateral MSON, only data from the nonaffected eye were used. Patients with a lesion volume of their OR exceeding the highest value observed in our control cohort were excluded. Controls were age matched to patients. The cutoff level for high serum lactate concentrations (2 mmol/L) was taken from a large reference population of 625 healthy control subjects.<sup>14</sup> Normality was tested graphically and using Shapiro–Wilk statistics. Because averaged data were used for both eye we did not perform generalized estimating equation (GEE) which corrects for intereye dependencies, instead data with normal distribution were compared using the *t* test. Correlation analyses were performed using Pearson's *R* for normally distributed and Spearman's *R* for non-Gaussian data. The Bonferroni method was used to correct for multiple correlations. Power calculations were performed using proc power in SAS with alpha set to 0.05.

## Results

### Study cohort void of MS lesions in visual pathways

We identified 31 patients with MS who did have no clinical or radiological evidence for either MSON or lesions within their optic radiations. This corresponds to 31/230 (13.5%) of our original cohort.<sup>7</sup> The demographic data of the patients are summarized in Table 1. The groups were matched for age, but there were more female patients compared to healthy control subjects ( $P < 0.01$ ).

The serum lactate levels were significantly higher in patients with MS compared to control subjects (Table 1,  $P = 0.029$ ). Importantly, serum lactate levels were not correlated with either age ( $P = 0.23$ ), age at onset ( $P = 0.42$ ), or disease duration ( $P = 0.37$ ).

### Dominant dyschromatopsia in MS

Color vision was impaired in 20/24 (83.3%) and typical for an acquired loss of color vision.<sup>20</sup> High contrast VA averaged at 0.9 with a mode of 1.0 (Table 2). Fourteen patients had a VA >1.0 and only 3/31 (9.7%) had a VA <0.8. Color vision was significantly more frequently impaired compared to high contrast VA ( $\chi^2 P = 0.01$ ).

### Structural relationships

In patients with high serum lactate levels there was significantly more retinal layer atrophy of the pRNFL ( $P = 0.041$ ,

**Table 1.** Subject characteristics.

|                  | Controls     | MS patients              |
|------------------|--------------|--------------------------|
| Subjects         | 31           | 31                       |
| Gender (m:f)     | 15:16        | 5:26 <sup>1</sup>        |
| Age (years)      | 53.2 (5.6)   | 55.1 (10.5) <sup>2</sup> |
| Age at onset     | n/a          | 37.6 (8.4)               |
| Disease duration | n/a          | 17.5 (6.3)               |
| EDSS             | n/a          | 3.7 (1.7)                |
| Disease course   | n/a          | 20 RR, 6 PP, 5 SP        |
| No MSON          | 31/31 (100%) | 21/31 (68%) <sup>3</sup> |
| MSON OD          | 0/31 (0%)    | 7/31 (23%) <sup>4</sup>  |
| MSON OS          | 0/31 (0%)    | 3/31 (10%) <sup>5</sup>  |
| Eyes included    | 62           | 52 <sup>6</sup>          |
| Serum lactate    | 2.39 (0.82)  | 2.81 (0.89) <sup>7</sup> |

The mean (SD), *n* (%) are shown. The disease course is indicated as RR, relapsing remitting; SP, secondary progressive; PP, primary progressive. MS, multiple sclerosis; EDSS, Expanded Disability Status Scale score; MSON, MS associated optic neuritis.

<sup>1</sup>Significantly more female subjects with MS compared to controls (chi-square test,  $P = 0.007$ ).

<sup>2</sup>Statistically no significant difference.

<sup>3</sup>OCT data from both eyes were averaged.

<sup>4</sup>Only OCT data OS (the nonaffected eye).

<sup>5</sup>Only OCT data OD (the nonaffected eye).

<sup>6</sup>OCT data from the 10 eyes with MSON were excluded.

<sup>7</sup> $P = 0.0294$ .

**Table 2.** Visual function in MS patients for the pooled cohort and dichotomized according to serum lactate levels.

|                   | MS patients   |                     |                          |
|-------------------|---------------|---------------------|--------------------------|
|                   | Pooled        | With normal lactate | With high lactate        |
| Visual acuity     | 0.90 (0.10)   | 0.94 (0.08)         | 0.91 (0.12)              |
| Confusion index   | 1.45 (0.42)   | 1.20 (0.19)         | 1.54 (0.45) <sup>1</sup> |
| Selectivity index | 1.83 (0.46)   | 1.61 (0.19)         | 1.90 (0.50)              |
| Confusion angle   | 51.54 (43.82) | 63.49 (5.29)        | 47.55 (50.22)            |

Data are shown for high contrast visual acuity and color vision as mean (SD) or number (%). MS, multiple sclerosis.

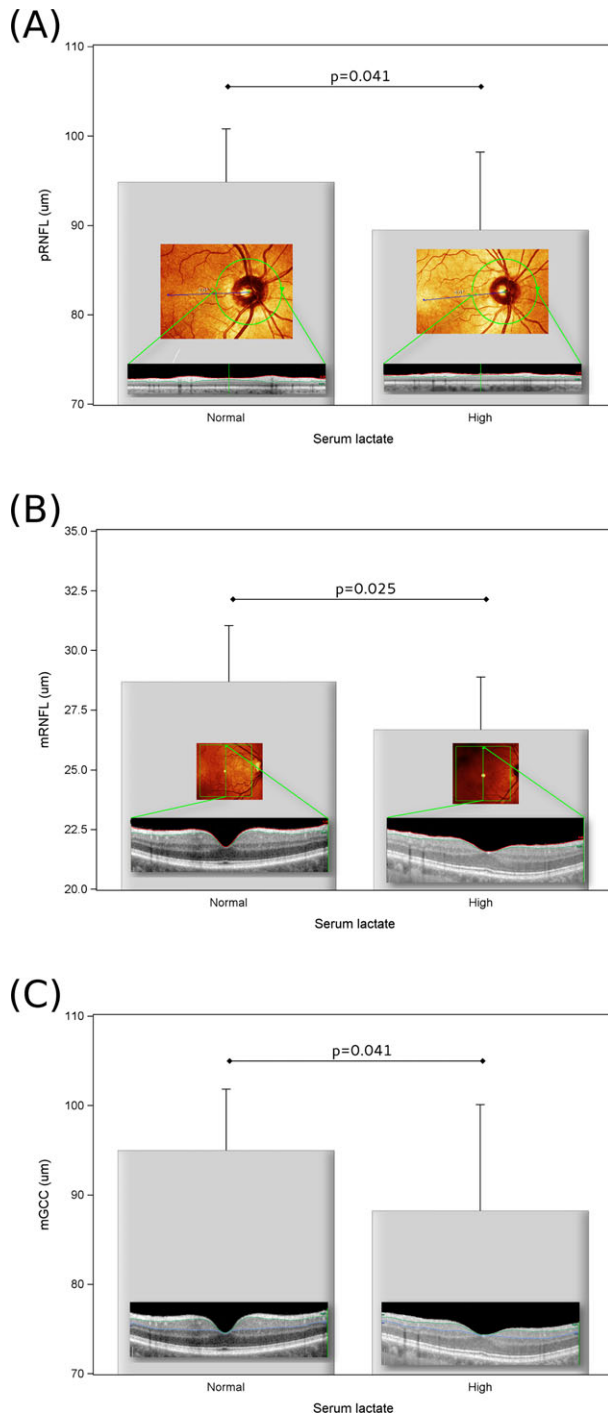
<sup>1</sup>Significantly more errors in MS patients with high serum lactate compared to MS patients with normal serum lactate ( $P = 0.0096$ ).

Fig. 2A), mRNFL ( $P = 0.025$ , Fig. 2B), and mGCC ( $P = 0.041$ , Fig. 2C) compared to those with normal serum lactate levels.

There was a trend for more severe cortical thinning in patients with high compared to normal serum lactate levels, but significance was narrowly missed ( $P = 0.061$ ).

### Functional relationships

Patients with high serum lactate levels had significantly more severe impairment of their color vision (confusion



index) compared to those with normal serum lactate levels (Table 2, Fig. 3,  $P < 0.01$ ).

Serum lactate levels were significantly correlated with clinical scales (Fig. 4). The correlation was strongest for the 9HPT (Pearson  $R = 0.53$ ,  $P = 0.002$ ), followed by the MSWS (Pearson  $R = 0.50$ ,  $P = 0.009$ ), EDSS (Spearman's  $R = 0.37$ ,  $P = 0.041$ ), and GNDS (Pearson  $R = 0.38$ ,

**Figure 2.** (A) There was more atrophy of the peripapillary RNFL (pRNFL) in patients with MS who have high serum lactate levels if compared to those with normal serum lactate levels. The inset shows representative images from two patients with MS included. The location of the peripapillary ring scan OD (commonly used abbreviation for latin *oculus dexter*, meaning right eye) is illustrated by the green circle in the confocal scanning laser ophthalmoscopic image. The segmented pRNFL is shown as the bright area between the red and green lines in the OCT image. The averaged pRNFL was 102 μm on the left (serum lactate 1.92 mmol/L) and 72 μm on the right (serum lactate 2.94 mmol/L). (B) There was more atrophy of the macular RNFL (mRNFL) in patients with MS who have high serum lactate levels if compared to those with normal serum lactate levels. The inset shows representative images from two patients with MS included. The area of the macular volume scan OD is illustrated by the green box in the confocal scanning laser ophthalmoscopic image. The green vertical arrow indicates the location of the OCT scan. The segmented mRNFL is shown as the bright area between the red and green lines in the OCT image. The averaged mRNFL was 32.25 μm on the left (serum lactate 1.86 mmol/L) and 23.5 μm on the right (serum lactate 3.61 mmol/L). (C) There was more atrophy of the macular GCC (mGCC) in patients with MS who have high serum lactate levels if compared to those with normal serum lactate levels. The inset shows the same OCT scan OD as in (B) with the segmented mGCC between the green and blue lines. The averaged mGCC was 105.75 μm on the left and 71.25 μm on the right. The mean and standard deviation are shown. RNFL, retinal nerve fiber layer; MS, multiple sclerosis; GCC, ganglion cell complex.

$P = 0.037$ ). Statistical significance remained for the 9HPT and MSWS after correcting for multiple ( $n = 4$ ) correlations with a corresponding Bonferroni corrected  $P$ -value of ( $0.0125 = 0.05/4$ ).

### Impaired lactate production and transport in MS lesions

Chronic active MS lesions were characterized by demyelination (Fig. 5A) and a rim of activated microglia and macrophages (Fig. 5B). Immunohistochemical analysis indicated that the lactate-generating enzyme LDHA was predominantly expressed by astrocytes throughout the normal appearing white matter (Fig. 5C). The expression of LDHA was markedly increased in MS lesions compared to normal appearing white matter. Interestingly, LDHA expression localized predominantly to large reactive astrocytes (Fig. 5D). Next, the lactate transporter MCT1 was highly expressed on blood-vessels and astrocyte processes throughout the normal appearing white matter (Fig. 5E) and lesions (Fig. 5F).<sup>25</sup>

### Discussion

This study proposed an in vivo model suitable to test systemic hypotheses on primary neurodegeneration in MS. The combination of clinical and MRI data permits to

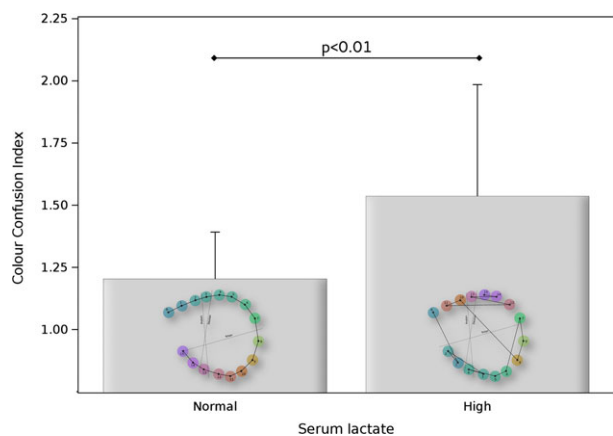


**Figure 3.** Color vision was more impaired in patients with multiple sclerosis (MS) who have high serum lactate levels if compared to those with normal serum lactate levels. A color confusion index of 1.00 indicates a perfect test result from a patient with normal lactate levels (0.96 mmol/L) and illustrated as inset to the left box. The result from a patient with impaired color vision (confusion index 2.50) and high lactate levels (3.44 mmol/L) is shown as inset to the right box. The blue colored reference cap is indicated as "R". Dashed lines indicate directions of confusion typically found for protanomals, deuteranomals, and tritanomals. The pattern of confusion (closed lines on the right) are characteristic for an acquired color deficit. The mean and standard deviation are shown.

describe a subgroup of patients with MS in which there is no MRI evidence for MS lesions within the visual pathways. These patients should therefore not suffer from inner retinal layer atrophy secondary to bidirectional trans-synaptic axonal degeneration caused by MS lesions of the visual pathways.<sup>6,7</sup> Consequently, using retinal OCT as a highly accurate quantitative readout<sup>10,23,27</sup> for this in vivo model permits to specifically test for other mechanisms thought responsible for neurodegeneration in MS.<sup>11</sup>

The main finding using this novel visual pathway model was to provide indirect biomarker evidence that mitochondrial dysfunction was related to neurodegeneration, both structurally and functionally. The biomarker chosen was lactate because it reflects on mitochondrial dysfunction which is considered a key feature of neurodegeneration in MS (Fig. 1). Consistent with previous data, serum lactate levels in this study were significantly higher in patients with MS compared to healthy controls.<sup>14,28</sup> Because of the high lipid content of the brain it is interesting noting recent adipous tissue microdialysis data in MS.<sup>29</sup> Extracellular fluid lactate levels in MS were higher at baseline and significantly increased with exercise if compared to control levels.<sup>29</sup> Such changes were not observed for muscle tissue.<sup>29</sup>

Structurally, the extent of atrophy in MS patients with high serum lactate levels exceeded what can be seen by

physiological variation alone.<sup>30,31</sup> However, the need for OCT QC using validated criteria cannot be overemphasized because the observed group differences fall in the range of known measurement artefacts.<sup>24</sup>

Functionally, the significant loss of color vision was associated with higher serum lactate levels. Consistent with this finding elevated serum lactate levels were also related to more extensive loss of function on global scales (EDSS, GNDS), upper limb function (9HPT), and lower limb function (MSWS). The scales used have complementary strength lending more weight to the overall correlative evidence.

A strength of this study was the long disease duration which might have facilitated demonstrating the structural and functional relationships with serum lactate in MS. This advantage was counter balanced by the smaller number of patients, corresponding to only 15.5% of our original cohort.<sup>7,21</sup> This seems inevitable given the high prevalence of optic pathway involvement in MS.<sup>18</sup> This may also turn out to be the practical challenge of the proposed model for clinical patient recruitment. Power calculations on the present data illustrate the actual power of the present study and how many patients would be needed for each of the three OCT readouts used (Table 3). An interesting observation from these power calculations is that test of function (color vision) performs better than test of structure (OCT). This is interesting because color vision relies on cones which have a higher metabolic demand compared to rods.<sup>32</sup> In addition, foveal cone signaling has to pass through an anatomical vulnerable structure, the foveal fibers, also known as the papillomacular bundle.<sup>33</sup> Finally, acquired loss of color vision can now be assessed with high accuracy, using state-of-the art, age adjusted, computerized color vision tests.<sup>34,35</sup> Such methods will be required for future longitudinal studies relating quantitative data on color vision to structural imaging data on integrity of the retina and visual pathways, genetic and body fluid biomarker data.

It has long been recognized that the axons constituting the papillomacular bundle are particularly vulnerable.<sup>36</sup> This might in part be related to their small diameter. Electron-microscopic studies in primates show a diameter of around 0.4  $\mu\text{m}$  for the papillomacular bundle with a complete lack of the larger 2.5  $\mu\text{m}$  fibers seen elsewhere in the retina.<sup>37</sup> Naturally, there are less mitochondria in thinner fibers compared to thicker fibers limiting energy resources by unchanged energy requirements to maintain axonal conduction.<sup>38</sup> The size-dependent differences in axonal susceptibility to degeneration have since been corroborated in a human postmortem study using histochemistry.<sup>39</sup> This study demonstrated predominant loss of the parvocellular layer of the lateral geniculate nucleus

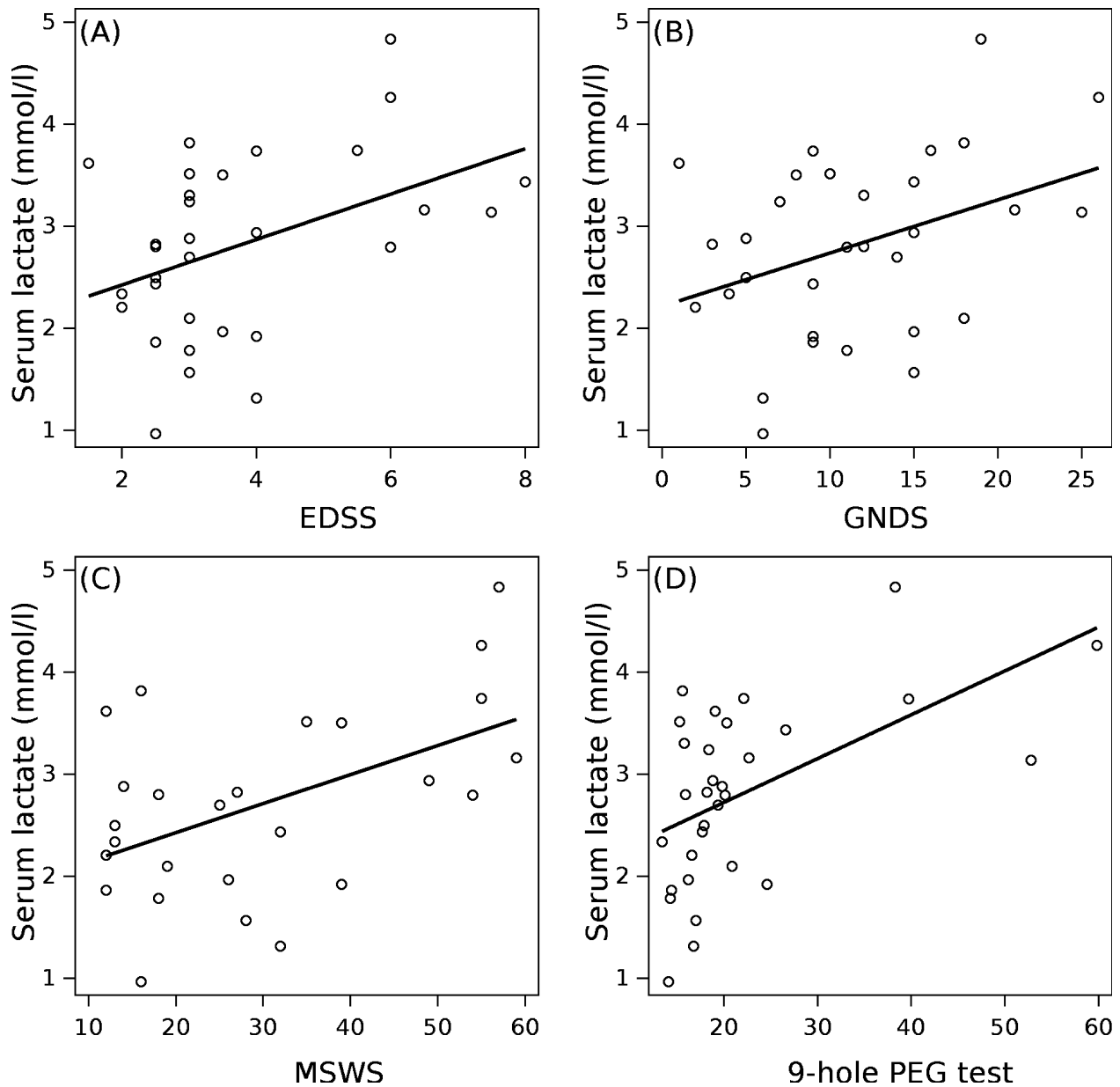


**Figure 4.** Serum lactate levels correlated with the (A) EDSS ( $R = 0.37$ ,  $P = 0.041$ ), (B) GNDS ( $R = 0.38$ ,  $P = 0.037$ ), (C) MSWS ( $R = 0.50$ ,  $P = 0.009$ ) and (D) 9-hole PEG test ( $R = 0.53$ ,  $P = 0.002$ ). EDSS, Expanded Disability Status Scale score; GNDS, Guy's Neurological Disability Scale; MSWS-12, Multiple Sclerosis Walking Scale.

which represents the smaller sized retinal axons.<sup>39</sup> Importantly, neurons of the parvocellular pathway are particularly involved in color vision. In this context, our findings indirectly support the clinical observation of a progressive optic neuropathy in a very small proportion of patients with MS from the pregenetic and pre-MRI area.<sup>40,41</sup> Already Parinaud reported slowly progressive dyschromatopsia in MS.<sup>41</sup> Later, Ashworth reported nine cases with insidious and progressive visual failure out of a series of 15 patients with presumed chronic

retrobulbar and chiasmal neuritis. Dyschromatopsia was not systematically investigated but scotoma to red targets reported in two cases (#7 & #9).<sup>40</sup>

Extending from the visual system to a more global assessment of the brain, this study narrowly failed to demonstrate a statistical relationship between serum lactate levels and gray matter atrophy ( $P = 0.06$ ). A limitation here is the sample size as further illustrated by the power calculations (Table 3). A possible explanation might be that the spatial resolution of MRI is lower com-

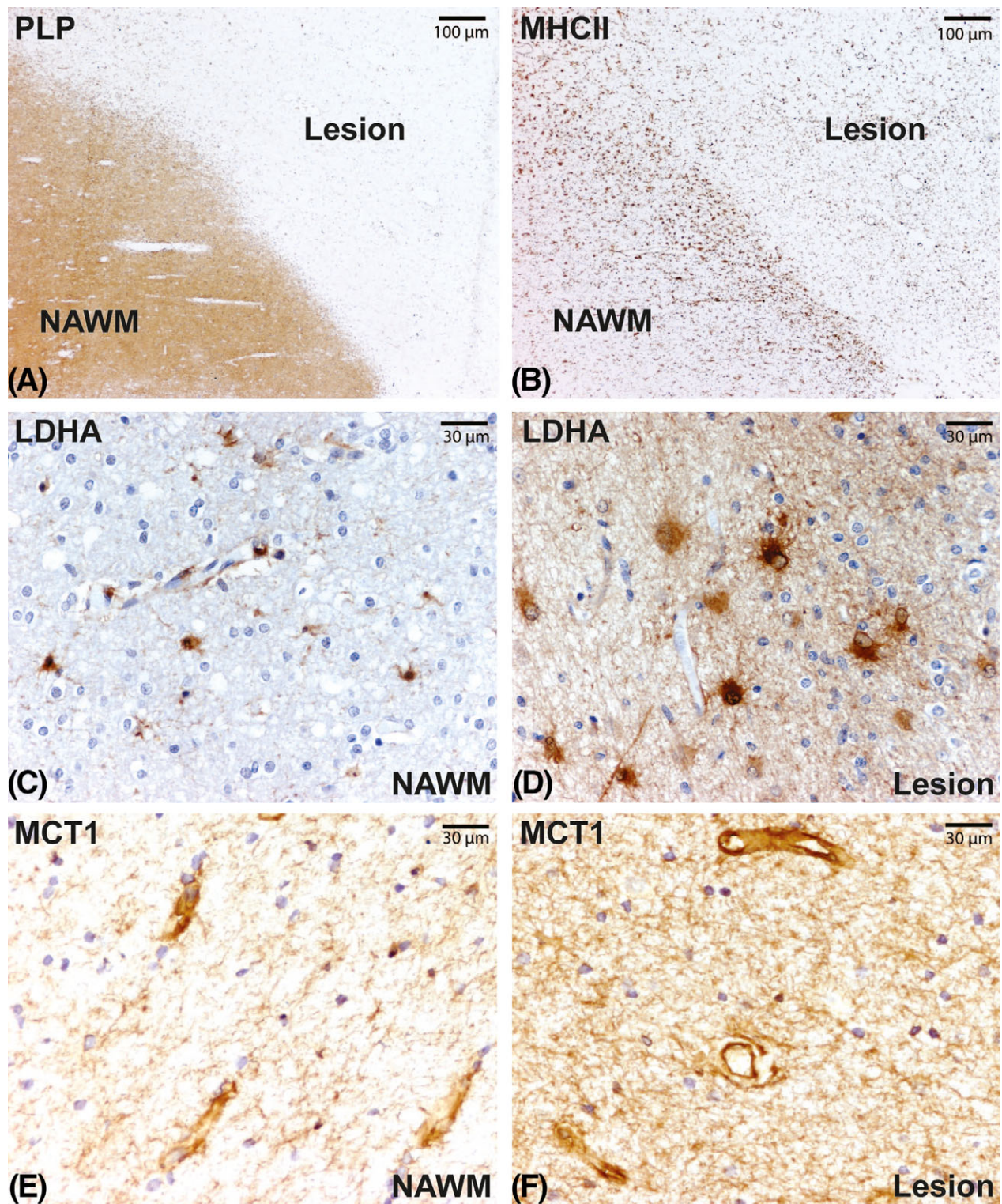


**Figure 5.** Chronic active MS lesions are characterized by loss of proteolipid protein (PLP, A) and a rim of activated MHCII positive microglia and macrophages (B). LDHA staining intensity is increased in MS lesions (D) compared to normal appearing white matter (C). MCT1 is highly expressed on blood-vessels in both normal appearing white matter (E) and lesions (F). MS, multiple sclerosis; LDHA, lactate dehydrogenase A; MCT, monocarboxylate transporter 1.



**Table 3.** Sample sizes required to test systemic hypotheses of neurodegeneration on the suggested optic pathway model using structural (OCT) and functional (color vision) readouts.

| Readout                 | Actual power | Desired power | Numbers needed |
|-------------------------|--------------|---------------|----------------|
| OCT pRNFL               | 41%          | 80%           | $n = 72$       |
| OCT mRNFL               | 43%          | 80%           | $n = 72$       |
| OCT mGCC                | 41%          | 80%           | $n = 68$       |
| MRI GM<br>(Grey matter) | 33%          | 80%           | $n = 74$       |
| Color vision            | 67%          | 80%           | $n = 36$       |

Power calculations were based on  $\alpha = 0.05$  for a two-sample *t* Test. pRNFL, peripapillary retinal nerve fiber layer; mRNFL, macular RNFL; mGCC, macular ganglion cell complex.

pared to OCT and that imaging of the cortical gray matter remains technically difficult.<sup>42</sup> For both reasons MRI data may be more noisy compared to OCT data in this particular context.

Next, we studied the cellular distribution of the lactate generating enzyme LDHA and monocarboxylate transporter-1 (MCT-1), which is the main lactate transporter in well-characterized MS brain tissue samples. The data suggest that enhanced levels of the lactate-producing enzyme LDHA in combination with marked endothelial lactate transporters in MS lesions might contribute to increased lactate levels. Future studies aimed to investigate the link of the present biomarker data with pathological studies of the eye and anterior visual pathways will need to consider cell type specific metabolic pathways as well as relevant transporters.<sup>25</sup> Such future studies should also consider adipous tissue as a likely source for systemic lactate levels based on microdialysis data.<sup>29</sup>

There are other limitations of this study which need to be discussed. Anatomically there is large variability of the retinal axonal projections through the optic radiations with relevant right left asymmetry.<sup>43</sup> Despite state of the art MRI tractography currently used in the field,<sup>4</sup> not all retino-cortical projections will be captured. MR spectroscopy and quantitative MRI metrics will be required to investigate more diffuse pathology.<sup>44,45</sup> Next, it is not clear if all radiological white matter lesions are relevant. Radiological signal changes of the white matter increase with age and were clearly seen in the present healthy control group. The chosen pragmatic approach to use a quantitative cut-off for the white matter lesion volume based on the control group might need qualitative refinements. Our 3T MRI protocol is very sensitive for detection of MS lesions, however, ultrahighfield MR might be even better suited to separate MS plaques from other white matter signal changes.<sup>4,44,46</sup> Certainly, much more data will be required on visual function, including testing for low contrast sensitivity, dyschromatopsia and electrophysiology.<sup>34,35,47,48</sup> The full spectrum of psychophysiological testing has not

yet been exploited, possibly dynamic visual tests are a step in this direction, suitable for quantitative, longitudinal readouts.<sup>49</sup> Finally lactate can be elevated for a number of reasons we have discussed in detail.<sup>14</sup> In the current cohort there was no clinical evidence to suggest an inclusion bias to the high lactate group due to systemic infection, muscle atrophy, or deconditioning.

A limitation of the study design was that we were unable to say whether the here observed subtle impairment of mitochondrial function might already play a role in patients with clinically isolated syndromes. The literature suggests that if lesions to the visual pathways are excluded, no pRNFL atrophy was observed in clinical isolated syndromes.<sup>50,51</sup> There is rather conflicting data on macular volume on a group level and confirmation of these data in a longitudinal study, excluding lesions in the visual pathways, is awaited.<sup>50,52,52,53</sup>

In conclusion, this study describes a visual pathway model suitable to test systemic and genetic hypotheses on pathways of neurodegeneration in MS.<sup>11</sup> The biomarker data suggests that there are structural and functional relationship of mitochondrial dysfunction and primary neurodegeneration in long-standing MS. There is a need for neuroprotective studies aimed to improve mitochondrial function, but results have been conflicting so far.<sup>1</sup> The sample size calculations on the here described visual pathway model, void of MS lesions, suggest that future studies to clarify these burning issues are feasible.

## Acknowledgment

The MS Center VUMC is partially funded by a program grant of the Dutch MS Research Foundation (grant 09-358d MS). This work has partly been funded by the Catholic University of Rome and the University of Catania. Shipment of samples has been privately sponsored by A. P. The authors' work described in this paper is supported by the University College London Comprehensive Biomedical Research Centre and the Moorfields Biomedical Research Centre.

## Conflict of Interest

Dr. Petzold reports personal fees from Novartis, not related to the submitted work. Dr. Wattjes reports personal fees from Biogen Idec, outside the submitted work.

## References

1. Maghzi A-H, Minagar A, Waubant E. Neuroprotection in multiple sclerosis: a therapeutic approach. *CNS Drugs* 2013;27:799–815.
2. Trapp B, Peterson J, Ransohoff RM, et al. Axonal transection in the lesions of multiple sclerosis. *N Engl J Med* 1998;338:278–285.

3. Jindahra P, Petrie A, Plant GT. Retrograde trans-synaptic retinal ganglion cell loss identified by optical coherence tomography. *Brain* 2009;132:628–634.
4. Klistorner A, Sriram P, Vootakuru N, et al. Axonal loss of retinal neurons in multiple sclerosis associated with optic radiation lesions. *Neurology* 2014;82:2165–2172.
5. Gabilondo I, Martínez-Lapiscina EH, Martínez-Heras E, et al. Trans-synaptic axonal degeneration in the visual pathway in multiple sclerosis. *Ann Neurol* 2014;75:98–107.
6. Balk LJ, Steenwijk MD, Tewarie P, et al. Bidirectional trans-synaptic axonal degeneration in the visual pathway in multiple sclerosis. *J Neurol Neurosurg Psychiatry* 2014; [Epub ahead of print].
7. Balk LJ, Twisk JWR, Steenwijk MD, et al. A dam for retrograde axonal degeneration in multiple sclerosis? *J Neurol Neurosurg Psychiatry* 2014;85:782–789.
8. Costello FE, Klistorner A, Kardon R. Optical coherence tomography in the diagnosis and management of optic neuritis and multiple sclerosis. *Ophthalmic Surg Lasers Imaging* 2011;42(suppl):S28–S40.
9. Zimmermann H, Freing A, Kaufhold F, et al. Optic neuritis interferes with optical coherence tomography and magnetic resonance imaging correlations. *Mult Scler* 2013;19:443–450.
10. Petzold A, de Boer JF, Schippling S, et al. Optical coherence tomography in multiple sclerosis: a systematic review and meta-analysis. *Lancet Neurol* 2010;9:921–932.
11. Friese MA, Schattling B, Fugger L. Mechanisms of neurodegeneration and axonal dysfunction in multiple sclerosis. *Nat Rev Neurol* 2014;10:225–238.
12. Lassmann H, van Horssen J, Mahad D. Progressive multiple sclerosis: pathology and pathogenesis. *Nat Rev Neurol* 2012;8:647–656.
13. Witte ME, Mahad DJ, Lassmann H, van Horssen J. Mitochondrial dysfunction contributes to neurodegeneration in multiple sclerosis. *Trends Mol Med* 2014;20:179–187.
14. Amorini AM, Nociti V, Petzold A, et al. Serum lactate as a novel potential biomarker in multiple sclerosis. *Biochim Biophys Acta* 2014;1842:1137–1143.
15. Choi J, Chandrasekaran K, Demarest TG, et al. Brain diabetic neurodegeneration segregates with low intrinsic aerobic capacity. *Ann Clin Transl Neurol* 2014;1:589–604.
16. Costello FE. Optical coherence tomography technologies: which machine do you want to own? *J Neuroophthalmol* 2014;34(suppl):S3–S9.
17. McDonald W, Compston A, Edan G, et al. Recommended diagnostic criteria for multiple sclerosis: guidelines from the International Panel on the diagnosis of multiple sclerosis. *Ann Neurol* 2001;50:121–127.
18. Petzold A, Wattjes MP, Costello F, et al. The investigation of acute optic neuritis: a review and proposed protocol. *Nat Rev Neurol* 2014;10:447–458.
19. Lublin F, Reingold S. Defining the clinical course of multiple sclerosis: results of an international survey. National Multiple Sclerosis Society (USA) Advisory Committee on Clinical Trials of New Agents in Multiple Sclerosis. *Neurology* 1996;46:907–911.
20. Vingrys AJ, King-Smith PE. A quantitative scoring technique for panel tests of color vision. *Invest Ophthalmol Vis Sci* 1988;29:50–63.
21. Balk L, Tewarie P, Killestein J, et al. Disease course heterogeneity and OCT in multiple sclerosis. *Mult Scler* 2014;20:1198–1206.
22. Artiss JD, Karcher RE, Cavanagh KT, et al. A liquid-stable reagent for lactic acid levels. Application to the Hitachi 911 and Beckman CX7. *Am J Clin Pathol* 2000;114:139–143.
23. Balk LJ, Petzold A. Influence of the eye-tracking-based follow-up function in retinal nerve fiber layer thickness using Fourier-domain optical coherence tomography. *Invest Ophthalmol Vis Sci* 2013;54:3045.
24. Schippling S, Balk L, Costello F, et al. Quality control for retinal OCT in multiple sclerosis: validation of the OSCAR-IB criteria. *Mult Scler* 2014; [Epub ahead of print].
25. Nijland PG, Michailidou I, Witte ME, et al. Cellular distribution of glucose and monocarboxylate transporters in human brain white matter and multiple sclerosis lesions. *Glia* 2014;62:1125–1141.
26. Witte ME, Nijland PG, Drexhage JAR, et al. Reduced expression of PGC-1 $\alpha$  partly underlies mitochondrial changes and correlates with neuronal loss in multiple sclerosis cortex. *Acta Neuropathol* 2013;125:231–243.
27. Balk LJ, Petzold A. Current and future potential of retinal optical coherence tomography in multiple sclerosis with and without optic neuritis. *Neurodegener Dis Manag* 2014;4:165–176.
28. Hansen D, Wens I, Keytsman C, et al. Is long-term exercise intervention effective to improve cardiac autonomic control during exercise in subjects with multiple sclerosis? A randomized controlled trial. *Eur J Phys Rehabil Med* 2014 [Epub ahead of print].
29. Mähler A, Steiniger J, Bock M, et al. Is metabolic flexibility altered in multiple sclerosis patients? *PLoS One* 2012;7:e43675.
30. Balk LJ, Sonder JM, Strijbis EMM, et al. The physiological variation of the retinal nerve fiber layer thickness and macular volume in humans as assessed by spectral domain-optical coherence tomography. *Invest Ophthalmol Vis Sci* 2012;53:1251–1257.
31. Balk L, Mayer M, Uitdehaag B, Petzold A. Physiological variation of segmented OCT retinal layer thicknesses is short-lasting. *J Neurol* 2013;260:3109–3114.
32. Perkins GA, Ellisman MH, Fox DA. Three-dimensional analysis of mouse rod and cone mitochondrial cristae architecture: bioenergetic and functional implications. *Mol Vis* 2003;9:60–73.

33. Plant GT, Perry VH. The anatomical basis of the caecocentral scotoma. New observations and a review. *Brain* 1990;113(Pt 5):1441–1457.
34. Rodriguez-Carmona M, O'Neill-Biba M, Barbur JL. Assessing the severity of color vision loss with implications for aviation and other occupational environments. *Aviat Space Environ Med* 2012;83:19–29.
35. Barbur JL, Konstantakopoulou E. Changes in color vision with decreasing light level: separating the effects of normal aging from disease. *J Opt Soc Am A Opt Image Sci Vis* 2012;29:A27–A35.
36. Uththoff W. Untersuchungen über den Einfluss des chronischen Alkoholismus auf das menschliche Sehorgan. *Arch Ophthalmol* 1886;32:95–188.
37. Ogden TE. Nerve fiber layer of the primate retina: morphometric analysis. *Invest Ophthalmol Vis Sci* 1984;25:19–29.
38. Sadun AA, La Morgia C, Carelli V. Mitochondrial optic neuropathies: our travels from bench to bedside and back again. *Clin Experiment Ophthalmol* 2013;41:702–712.
39. Evangelou N, Konz D, Esiri MM, et al. Size-selective neuronal changes in the anterior optic pathways suggest a differential susceptibility to injury in multiple sclerosis. *Brain* 2001;124:1813–1820.
40. Ashworth B. Chronic retrobulbar and chiasmal neuritis. *Br J Ophthalmol* 1967;51:698.
41. Parinaud H. Troubles oculaires de la sclérose en plaques. *Prog Méd (Paris)* 1884;12:641–650.
42. Chard DT, Parker GJM, Griffin CMB, et al. The reproducibility and sensitivity of brain tissue volume measurements derived from an SPM-based segmentation methodology. *J Magn Reson Imaging* 2002;15:259–267.
43. Jeelani NUO, Jindahra P, Tamber MS, et al. 'Hemispherical asymmetry in the Meyer's Loop': a prospective study of visual-field deficits in 105 cases undergoing anterior temporal lobe resection for epilepsy. *J Neurol Neurosurg Psychiatry* 2010;81:985–991.
44. Wattjes MP, Harzheim M, Lutterbey GG, et al. High field MR imaging and 1H-MR spectroscopy in clinically isolated syndromes suggestive of multiple sclerosis: correlation between metabolic alterations and diagnostic MR imaging criteria. *J Neurol* 2008;255:56–63.
45. Pfueller CF, Brandt AU, Schubert F, et al. Metabolic changes in the visual cortex are linked to retinal nerve fiber layer thinning in multiple sclerosis. *PLoS One* 2011;6:e18019.
46. Sinnecker T, Oberwahrenbrock T, Metz I, et al. Optic radiation damage in multiple sclerosis is associated with visual dysfunction and retinal thinning – an ultrahigh-field MR pilot study. *Eur Radiol* 2014;25:122–131.
47. Balcer LJ, Baier ML, Cohen JA, et al. Contrast letter acuity as a visual component for the Multiple Sclerosis Functional Composite. *Neurology* 2003;61:1367–1373.
48. Schnurman ZS, Frohman TC, Beh SC, et al. Retinal architecture and mfERG: optic nerve head component response characteristics in MS. *Neurology* 2014;82:1888–1896.
49. Raz N, Hallak M, Ben-Hur T, Levin N. Dynamic visual tests to identify and quantify visual damage and repair following demyelination in optic neuritis patients. *J Vis Exp* 2014;(86). doi: 10.3791/51107.
50. Outteryck O, Zephir H, Defoort S, et al. Optical coherence tomography in clinically isolated syndrome: no evidence of subclinical retinal axonal loss. *Arch Neurol* 2009;66:1373–1377.
51. Oberwahrenbrock T, Ringelstein M, Jentschke S, et al. Retinal ganglion cell and inner plexiform layer thinning in clinically isolated syndrome. *Mult Scler* 2013;19:1887–1895.
52. Saidha S, Syc SB, Ibrahim MA, et al. Primary retinal pathology in multiple sclerosis as detected by optical coherence tomography. *Brain* 2011;134:518–533.
53. Khanifar AA, Parlitsis GJ, Ehrlich JR, et al. Retinal nerve fiber layer evaluation in multiple sclerosis with spectral domain optical coherence tomography. *Clin Ophthalmol* 2010;4:1007–1013.